# Thermal decomposition of humboldtine –a high resolution thermogravimetric and hot stage Raman spectroscopic study.

**R. L. Frost• and Matt L. Weier**

*Inorganic Materials Research Program, Queensland University of Technology, 2 George Street, Brisbane, GPO Box 2434, Queensland 4001, Australia.*

*Published as:*
Frost, R.L. and M.L. Weier, Thermal decomposition of humboldtine - a high resolution thermogravimetric and hot stage Raman spectroscopic study. Journal of Thermal Analysis and Calorimetry, 2004. 75(1): p. 277-291.

Copyright 2004 Springer

## Abstract

Evidence for the existence of primitive life forms such as lichens and fungi can be based upon the formation of oxalates. These oxalates form as a film like deposit on rocks and other host matrices. Humboldtine as the natural iron(II) oxalate mineral is a classic example. Thermogravimetry coupled to evolved gas mass spectrometry shows dehydration takes place in two steps at 130 and 141 °C. Loss of the oxalate as carbon dioxide occurs at 312 and 332 °C. Dehydration is readily followed by Raman microscopy in combination with a thermal stage and is observed by the loss of intensity of the OH stretching vibration at 3318 $cm^{-1}$. The application of infrared emission spectroscopy supports the results of the TG-MS. Three Raman bands are observed at 1470, 1465 and 1432 $cm^{-1}$ attributed the CO symmetric stretching mode. The observation of the three bands supports the concept of multiple iron(II) oxalate phases. The significance of this work rests with the ability of Raman spectroscopy to identify iron(II)oxalate which often occurs as a film on a host rock.

**Keywords:** oxalate, humboldtine, high resolution thermogravimetric analysis, hot stage Raman spectroscopy, infrared emission spectroscopy

## Introduction

The presence of oxalates is widespread in nature. These minerals form as the result of expulsion of heavy metals from fungi, lichens and plants [1-3]. The production of simple organic acids such as oxalic and citric acids has profound implications for metal speciation in biogeochemical cycles [4]. The metal complexing properties of the acids are essential to the nutrition of fungi and lichens and affects the metal stability and mobility in the environment [4]. Lichens and fungi produce the oxalates of heavy metals as a mechanism for the removal of heavy metals from the plant [5]. Humboldtine was identified as a mineral many years ago [6] and its structure was determined [7-9]. Stacking faults in iron(II) oxalates has been determined [10, 11].

• Author to whom correspondence should be addressed (r.frost@qut.edu.au)

Recently Macnish and others identified intracellular calcium oxalate crystals in Geraldton wax flowers (*Chamelaucium uncinatum*). These authors considered that the complexation of the oxalic acid with calcium controlled the concentration of heavy metals in the plant. Importantly the crystals were < 1 micron in size and were very difficult to identify using techniques such as X-ray diffraction. Raman spectroscopy however proved useful for the analysis of the calcium oxalate. The presence of these oxalate crystals appears to have an effect similar to that found in cacti [12]. Among the oxalates are the two calcium oxalates known as weddellite (the dihydrate) and whewellite (monohydrate). Ca-oxalate exists in two well-described modifications: as the more stable monoclinic monohydrate whewellite and the less stable tetragonal dihydrate weddellite. Weddelite serves for lichens as a water absorbing and accumulating substrate which transforms to whewellite when humidity drops. Such minerals are important in human physiology as the minerals are found in urinary tracts [13, 14]. Many other divalent oxalates exist in nature. The magnesium based oxalate is known as glushinskite [15, 16]. The copper oxalate is known as moolooite [2, 17] and the iron(II) oxalate as humboldtine [6, 18]. These three oxalates are also the product of lichen growth. Two natural univalent oxalates are known. These are the oxalates of sodium and ammonium known as natroxalate and oxammite [19].

Indeed the presence of oxalates have been evidence for the deterioration of works of art [20-22]. Carbon dating of oxalic acid enables estimates of the age of the works of art [23]. The presence of the oxalates has been used as indicators of climate change [24]. The presence of pigments in ancient works of art effected the growth of lichens on the art works [25]. In calcareous artifacts such as the famous Chinese terra cotta soldiers or Egyptian epigraphs they lead to a destruction of the surface by forming Ca-oxalate layers and thus to a deterioration of the historian work of art. But in places where the surface is covered by some blue colours (Egyptian and Chinese Blue, Chinese Purple) the growth of lichens is inhibited and the artifacts are well preserved. The copper ion contained in the pigments is responsible for this effect since copper is a strong poison for micro-organisms [25]. Weddellite and whewellite very often occur together with gypsum on the surface of calcareous artifacts exposed in the Mediterranean urban environment, as main constituents of reddish patinas called in Italy 'scialbatura'. The origin of this is a matter of controversy. The observation of the interface between calcite substratum and the above mentioned secondary minerals is an important step in the explanation of alteration process of artifacts of historic and artistic interest [26]. Studies of the black paint has shown the presence of oxalates in the paint with serious implications for remediation [27]. The use of infrared and Raman spectroscopy for the study of oxalates originated with the necessity to study renal stones [28, 29]. FT Raman spectroscopy has been used to study urolithiasis disease that has been studied for many years, and the ethiopathogenesis of stone formation is not well understood [30].

Whilst there have been several studies of synthetic metal oxalates [31-37], few studies of natural oxalates have been forthcoming and few spectroscopic studies of the iron(II) natural oxalate has been undertaken. The objective of this work is to undertake a comparative study using a combination of Raman and infrared spectroscopy combined with a thermal stage

## EXPERIMENTAL

### 2.1 *Mineral*

The humboldtine (sample Number M13748 originated from Bohemia, Czech Republic) was obtained from the South Australian museum [18]. The sample was phase analyzed using X-ray diffraction and the compositions checked using EDX measurements.

### 2.2 *Thermal analysis*

Thermal decomposition of the natural oxalate was carried out in a TA® Instruments incorporated high-resolution thermogravimetric analyzer (series Q500) in a flowing nitrogen atmosphere (80 $cm^3$/min). Approximately 50mg of sample was heated in an open platinum crucible at a rate of 1.0 °C/min up to 500°C. The TGA instrument was coupled to a Balzers (Pfeiffer) mass spectrometer for gas analysis. Only selected gases were analyzed.

### *2.3 Raman microprobe spectroscopy*

The crystals humboldtine were placed and orientated on the stage of an Olympus BHSM microscope, equipped with 10x and 50x objectives and part of a Renishaw 1000 Raman microscope system, which also includes a monochromator, a filter system and a Charge Coupled Device (CCD). Raman spectra were excited by a HeNe laser (633 nm) at a resolution of 2 $cm^{-1}$ in the range between 100 and 4000 $cm^{-1}$. Repeated acquisition using the highest magnification was accumulated to improve the signal to noise ratio. Spectra were calibrated using the 520.5 $cm^{-1}$ line of a silicon wafer. In order to ensure that the correct spectra are obtained, the incident excitation radiation was scrambled. Previous studies by the authors provide more details of the experimental technique. Spectra at liquid nitrogen temperature were obtained using a Linkam thermal stage (Scientific Instruments Ltd, Waterfield, Surrey, England).

### *2.4 Infrared emission spectroscopy*

Details of infrared emission spectroscopy has been previously published [38-40]. Spectroscopic manipulation such as baseline adjustment, smoothing and normalisation were performed using the Spectracalc software package GRAMS (Galactic Industries Corporation, NH, USA). Band component analysis was undertaken using the Jandel 'Peakfit' software package, which enabled the type of fitting, function to be selected and allows specific parameters to be fixed or varied accordingly. Band fitting was done using a Gauss-Lorentz cross-product function with the minimum number of component bands used for the fitting process. The Gauss-Lorentz ratio was maintained at values greater than 0.7 and fitting was undertaken until reproducible results were obtained with squared correlations of $r^2$ greater than 0.995.

## RESULTS AND DISCUSSION

***Thermal analysis***

The HRTG and MS curves for humboldtine are shown in Figures 1 and 2 respectively. The TGA curve for this mineral is complex. Three stages with multiple steps are observed. The first step is observed with two mass losses at 130 and 141 °C. The second is a broad step centred upon 235 °C. The third stage consists of two mass losses at 312 and 332 °C. In harmony with the TG results, mass spectrometry shows the evolved water in two steps at 126 and 132 °C. The carbon dioxide is emitted over a broad temperature range commencing at 200 °C. Two MS carbon dioxide emission peaks are observed at 322 and 354 °C. The values obtained are in agreement with previously published data [41-45].

The proposed mass loss steps are as follows:

$FeC_2O_4.2H_2O \rightarrow FeC_2O_4.H_2O + H_2O \rightarrow FeC_2O_4 + H_2O$

$FeC_2O_4 \rightarrow FeO + CO + CO_2$

and

$FeC_2O_4 \rightarrow FeCO_3 + CO$

$FeCO_3 \rightarrow FeO + CO_2$

Based on the HRTG results it is suggested that the iron(II) oxalate looses water in the first stage in steps from the dihydrate to the monohydrate and then to the anhydrous compound. It is proposed that the iron(II) oxalate then decomposes in two path ways. The first pathway is the conversion of the iron(II) acetate to iron(II) oxide and carbon monoxide and carbon dioxide. Berbenni recently studied the reaction of lithium carbonate with ferric oxalate [44]. Such a oxalate was also incorporated into a layer double hydroxide and thermal studies undertaken [46]. Thermal studies of the naturally occurring mineral iron(II) oxalate are less well known. Recently studies have shown valuable information can be obtained by using a combination of thermal analysis and spectroscopic techniques[47-50]. In this work we use a combination of thermogravimetry and hot stage infrared emission and Raman spectroscopy to study the thermal decomposition of the natural mineral humboldtine.

***Raman spectroscopy***

The Raman spectra of the hydroxyl stretching region thermally treated humboldtine are shown in Figure 3. Humboldtine is iron(II) oxalate dihydrate. The spectra clearly show that the intensity of the OH stretching mode is lost at temperatures below 200 °C. The band is at 3318 $cm^{-1}$ at 25 °C and shifts to 3333 $cm^{-1}$ at 150 °C showing a red shift to the band with thermal treatment. The infrared emission spectra shown in Figure 4 support the Raman data from the thermal treatment of humboldtine. The IE spectra are noisy at the lower temperatures; nevertheless two bands may be identified at 3355 and 3147 $cm^{-1}$. In the TG experiment two closely overlapping mass loss steps are observed at 131 and 141 °C. The MS experiment shows three water vapour evolutions at 126, 132 and 141 °C. The results of the Raman and infrared emission spectroscopic studies are in harmony with the TG and MS results in that all four experiments show that there is no water remaining in the structure of the thermally treated humboldtine after 150 °C. The TG and MS experiments show at least two mass loss steps. Such steps were not observed in either the Raman or the IES experiment as the temperature intervals between

successive spectra were two large. It should be recognised that the band at 3318 $cm^{-1}$ in the Raman spectrum and the band at 3315 $cm^{-1}$ in the infrared emission spectrum are not attributable to the same vibrational mode. The former is ascribed to the OH symmetric stretching vibration and the latter to the OH antisymmetric stretching vibration. Figures 3 and 4 show somewhat conflicting information. The OH bands exist in the Raman spectrum at 150 °C; the intensity is low in the infrared emission spectrum at the same temperature. This difference is attributed to the lack of intensity in the infrared emission spectra at low temperatures. It is only at elevated temperatures that sufficient energy enables quality IE spectra to be obtained.

The Raman spectra of the CO stretching region are shown in Figure 5. Three bands are distinguished in the CO stretching region at 1470, 1465 and 1432 $cm^{-1}$. These bands are attributed to the CO symmetric stretching vibration. Low intensity bands are observed in the Raman spectra at 1709 and 1615 $cm^{-1}$. These bands may be attributed to the CO antisymmetric stretching vibration. The intensity of these Raman bands approaches zero by 150 °C. If the natural iron(II) oxalate was a single pure chemical then it might be expected that only a single CO stretching mode would be observed. Thermal treatment can cause the conversion of the humboldtine from the dihydrate to the monohydrate and then to the anhydrous iron(II) oxalate. The observation of three CO symmetric stretching vibrations provides credence to the existence of all three phases. Such a concept of the existence of all three phases is supported by the TG and MS results which show two distinct steps in the dehydration of the humboldtine.

The IE spectra of the 1100 to 2100 $cm^{-1}$ region of the thermally treated humboldtine are shown in Figure 6. The results of the infrared emission analyses are reported in Table 2. In the IE spectra at 25, 50 and 75 °C, intense bands are observed at 1629 $cm^{-1}$ and no bands are observed at around 1480 $cm^{-1}$. The band at 1629 $cm^{-1}$ is assigned to the CO antisymmetric stretching vibration. The band at around 1480 $cm^{-1}$ observed at higher temperatures is assigned to the 'forbidden' symmetric stretching vibration. At the lower temperatures the Raman and infrared spectra are mutually exclusive. This mutual exclusion is an indication of a centre of symmetry. Such a centre of symmetry would be achieved if the iron(II) oxalate was planar. Thermal treatment above 100 °C results in the loss of the mutual exclusion and hence it is concluded that the iron(II) oxalate is no longer planar but is distorted. It is probable that such distortion arises from stacking faults introduced through thermal treatment [10, 11].

The infrared spectra show quite intense bands centered around 1300 $cm^{-1}$. These bands may be assigned to $B_{3u}$ OCO stretching mode. The band is observed at 1315 $cm^{-1}$ for aqueous potassium oxalate and at 1313 $cm^{-1}$ for solid potassium oxalate. For weddellite and whewellite bands are observed at 1366 and 1309 $cm^{-1}$.A band was observed at 1365 $cm^{-1}$ and assigned to the OCO stretching mode for synthetic copper(II) oxalate dihydrate[51, 52]. Humboldtine shows a similar infrared pattern with component bands at 1312 and 1357 $cm^{-1}$. The IE spectra show intense bands at 1315 $cm^{-1}$ at 75 °C which occurs at 1306 $cm^{-1}$ at 375 °C before the intensity is lost. A second band is observed at 1360 $cm^{-1}$ and shows an increase in peak position with thermal treatment. The band is observed at 1367 $cm^{-1}$ at 375 °C. No bands are observed in these positions in the Raman spectra. It is probable that this latter band is attributable to the $B_2$ OCO wagging mode. The results of the IE spectra

are in harmony with the TG and MS results. IE spectra show that no intensity remains in the characteristic oxalate spectra after 375 °C. The TG results show that two mass loss steps are observed at 312 and 332 °C. The MS results prove the evolution of carbon dioxide at 322 and 354 °C in two mass loss steps. One possible mechanism is that at temperatures above 140 °C and below 322 °C, the anhydrous iron(II) oxalate is the decomposition product of humboldtine. At 322 °C the iron(II) oxalate changes from the bidentate to a mono-dentate ligand and at the second step at 354 °C, the mono-dentate oxalate ligand is lost.

The Raman spectra of the C-C stretching region of the thermally treated humboldtine are shown in Figure 7. The band is observed at 914 $cm^{-1}$ at 75 °C and shows a small blue shift with increasing temperature. Only a single C-C stretching vibration is observed. A second low intensity band is observed at 856 $cm^{-1}$ for humboldtine. The band is assigned to the OCO bending mode. A band is not observed in this position for potassium oxalate. The results of the Raman spectra of the thermal treatment of the humboldtine appear to be different from that of either the TG/MS data or the IES data. The loss of the oxalate seems to occur at significantly lower temperatures in the Raman thermal stage than in the IE stage. The infrared emission spectra of the 650 to 1100 $cm^{-1}$ region are shown in Figure 8. The first observation that can be made is that the C-C stretching mode is either not observed or is only weakly observed in the IE spectra. After thermal treatment of the humboldtine a very low intensity band is observed at around 913 $cm^{-1}$. It is possible that this is the infrared forbidden C-C stretching vibration. A low intensity band is observed at 943 $cm^{-1}$. A strong IE band is observed 819 $cm^{-1}$. The first band shows a strong red shift and the latter a blue shift with thermal treatment (Table 2). These bands are assigned to the OCO bending modes which are strong in the infrared spectrum and of low intensity in the Raman spectra.

The Raman spectra of the thermally treated humboldtine in the 200 to 700 $cm^{-1}$ region are shown in Figure 9. The spectra at 50, 100 and 150 °C are similar. Above 200 °C, the spectra are different and closely resemble the Raman spectrum of hematite. At 25 °C, bands are observed at 582 and 518 $cm^{-1}$. The bands are observed at 584 and 520 $cm^{-1}$ at 75 °C and show a slight blue shift up to 200 °C, after which the intensity is lost. Significant changes are observed in the very low wavenumber region of humboldtine before and after 200 °C. A set of bands are observed at 204, 244, 288 and 304 $cm^{-1}$. These bands may be assigned to MO stretching and OMO ring bending modes. At 200 °C, bands are observed at 219, 285, and 397 $cm^{-1}$. These bands correspond to the low wavenumber bands of hematite.

**Conclusions**

High resolution TG coupled to an evolved gas mass spectrometer shows that dehydration of humboldtine takes place in two stages at around 130 and 141 °C. Such two step dehydration supports the concept of iron(II) oxalate dihydrate changing to iron(II) monohydrate and then to the anhydrous iron(II) oxalate. Such a sequence is supported by the observation of three CO Raman bands. The thermal treatment of iron(II) oxalate was also studied by infrared emission spectroscopy. At low temperatures the infrared and Raman spectra are mutually exclusive; this supports the concept that the iron(II) oxalate is planar. At temperatures above the dehydration temperature this mutual exclusion is lost with the appearance in the infrared emission

spectra of a band at 1480 $cm^{-1}$. The IE spectra strongly support the loss of oxalate over the 275 to 375 temperature range.

If life existed on Mars at some time in the past or even exists in the present time, low life forms such as fungi and lichens may exist. Such organisms may be found in very hostile environments [53-55]. Lichens and fungi can control their heavy metal intake through expulsion as metal salts such as oxalates. The presence of these oxalates can be used as a marker for the pre-existence of life. Thus the study of the common natural oxalates is of great importance. The minerals on planets such as Mars may be explored by robotic devices which carry portable Raman spectrometers with perhaps fibre optics to collect spectral data. The interpretation of the spectra of natural oxalates is important for these types of studies.

**Acknowledgments**

The financial and infra-structure support of the Queensland University of Technology Inorganic Materials Research Program is gratefully acknowledged. The Australian Research Council (ARC) is thanked for funding. Mr Dermot Henry of Museum Victoria is thanked for the loan of the humboldtine mineral. is thanked for the loan of the oxalate minerals.

**References**

1. H. J. Arnott and M. A. Webb, Scanning Electron Microsc. (1983) 1747.
2. J. E. Chisholm, G. C. Jones and O. W. Purvis, Mineralogical Magazine 51 (1987) 715.
3. A. Frey-Wyssling, Am. J. Bot. 68 (1981) 130.
4. G. M. Gadd, Mineralogical Society Series 9 (2000) 57.
5. T. Wadsten and R. Moberg, Lichenologist 17 (1985) 239.
6. E. Manasse, Rend. accad. Lincei 19 (1911) 138.
7. F. Mazzi and C. Garavelli, Periodico mineral (Rome) 26 (1957) 269.
8. F. Mazzi and C. L. Garavelli, Periodico mineral. (Rome) 28 (1959) 243.
9. S. Caric, Bull. soc. franc. mineral. et crist. 82 (1959) 50.
10. H. Pezerat, J. Dubernat and J. P. Lagier, Comptes Rendus des Seances de l'Academie des Sciences, Serie C: Sciences Chimiques 288 (1968) 1357.
11. J. Dubernat and H. Pezerat, Journal of Applied Crystallography 7 (1974) 387.
12. P. V. Monje and E. J. Baran, Plant Physiology 128 (2002) 707.
13. J. P. Pestaner, F. G. Mullick, F. B. Johnson and J. A. Centeno, Archives of Pathology & Laboratory Medicine 120 (1996) 537.
14. J. Dubernat and H. Pezerat, J. Appl. Crystallogr. 7 (1974) 387.
15. H. Pezerat, J. Dubernat and J. P. Lagier, C. R. Acad. Sci., Paris, Ser. C 288 (1968) 1357.
16. M. J. Wilson and P. Bayliss, Mineralogical Magazine 51 (1987) 327.
17. R. M. Clarke and I. R. Williams, Mineralogical Magazine 50 (1986) 295.
18. K. Rezek, J. Sevcu, S. Civis and J. Novotny, Casopis pro Mineralogii a Geologii 33 (1988) 419.
19. H. Winchell and R. J. Benoit, Am. Mineralogist 36 (1951) 590.

20. A. Piterans, D. Indriksone, A. Spricis and A. Actins, Proceedings of the Latvian Academy of Sciences, Section B: Natural, Exact and Applied Sciences 51 (1997) 254.
21. M. Del Monte and C. Sabbioni, Environ. Sci. Technol. 17 (1983) 518.
22. M. Del Monte and C. Sabbioni, Science of the Total Environment 50 (1986) 165.
23. J. Girbal, J. L. Prada, R. Rocabayera and M. Argemi, Radiocarbon 43 (2001) 637.
24. S. Moore, M. J. Beazley, M. R. Mccallum and J. Russ, Preprints of Extended Abstracts presented at the ACS National Meeting, American Chemical Society, Division of Environmental Chemistry 40 (2000) 4.
25. I. Lamprecht, A. Reller, R. Riesen and H. G. Wiedemann, Journal of Thermal Analysis 49 (1997) 1601.
26. R. Alaimo and G. Montana, Neues Jahrbuch fuer Mineralogie, Abhandlungen 165 (1993) 143.
27. G. Alessandrini, L. Toniolo, F. Cariati, G. Daminelli, S. Polesello, A. Pozzi and A. M. Salvi, Studies in Conservation 41 (1996) 193.
28. H. Moenke, Chem. Erde 21 (1961) 239.
29. M. Daudon, M. F. Protat, R. J. Reveillaud and H. Jaeschke-Boyer, Kidney Int. 23 (1983) 842.
30. C. Paluszkiewicz, M. Galka, W. Kwiatek, A. Parczewski and S. Walas, Biospectroscopy 3 (1997) 403.
31. R. I. Bickley, H. G. M. Edwards and S. J. Rose, Journal of Molecular Structure 243 (1991) 341.
32. H. Chang and P. J. Huang, Analytical Chemistry 69 (1997) 1485.
33. D. Duval and R. A. Condrate, Sr., Applied Spectroscopy 42 (1988) 701.
34. H. G. M. Edwards, D. W. Farwell, R. Jenkins and M. R. D. Seaward, Journal of Raman Spectroscopy 23 (1992) 185.
35. I. I. Kondilenko, P. A. Korotkov, N. G. Golubeva, V. A. Klimenko and A. I. Pisanskii, Optika i Spektroskopiya 45 (1978) 819.
36. O. I. Kondratov, E. A. Nikonenko, I. I. Olikov and L. N. Margolin, Zhurnal Neorganicheskoi Khimii 30 (1985) 2579.
37. T. A. Shippey, Journal of Molecular Structure 63 (1980) 157.
38. R. L. Frost, Z. Ding, J. T. Kloprogge and W. N. Martens, Thermochimica Acta 390 (2002) 133.
39. R. L. Frost, Z. Ding, W. N. Martens and T. E. Johnson, Thermochimica Acta 398 (2003) 167.
40. R. L. Frost, J. Kristof, E. Horvath and J. T. Kloprogge, J. Raman Spectrosc. 32 (2001) 873.
41. J. Praharaj, S. K. Pati, S. C. Moharana and D. Bhatta, Journal of Teaching and Research in Chemistry 8 (2001) 4.
42. A. V. Shkarin, I. P. Suzdalev, B. M. Kadenatsi and G. M. Zhabrova, Khim. Vys. Energ. 2 (1968) 77.
43. B. S. Randhawa, Thermochimica Acta 254 (1995) 381.
44. V. Berbenni, A. Marini, G. Bruni and R. Riccardi, Thermochimica Acta 346 (2000) 115.
45. A. Coetzee, D. J. Eve and M. E. Brown, Journal of Thermal Analysis 39 (1993) 947.
46. S. Carlino and M. J. Hudson, Solid State Ionics 110 (1998) 153.

47. E. Horvath, J. Kristof, R. L. Frost, A. Redey, V. Vagvolgyi and T. Cseh, Journal of Thermal Analysis and Calorimetry 71 (2003) 707.
48. J. Kristof, R. L. Frost, J. T. Kloprogge, E. Horvath and E. Mako, Journal of Thermal Analysis and Calorimetry 69 (2002) 77.
49. J. Kristof, R. L. Frost, W. N. Martens and E. Horvath, Langmuir 18 (2002) 1244.
50. J. Kristof, E. Horvath, R. L. Frost and J. T. Kloprogge, Journal of Thermal Analysis and Calorimetry 63 (2001) 279.
51. H. G. M. Edwards and P. H. Hardman, Journal of Molecular Structure 273 (1992) 73.
52. H. G. M. Edwards and I. R. Lewis, Spectrochimica Acta, Part A: Molecular and Biomolecular Spectroscopy 50A (1994) 1891.
53. H. G. M. Edwards, E. M. Newton and J. Russ, Journal of Molecular Structure 550-551 (2000) 245.
54. H. G. M. Edwards, N. C. Russell, M. R. D. Seaward and D. Slarke, Spectrochimica Acta, Part A: Molecular and Biomolecular Spectroscopy 51A (1995) 2091.
55. H. G. M. Edwards, N. C. Russell and M. R. D. Seward, Spectrochimica Acta, Part A: Molecular and Biomolecular Spectroscopy 53A (1997) 99.

## LIST OF FIGURES

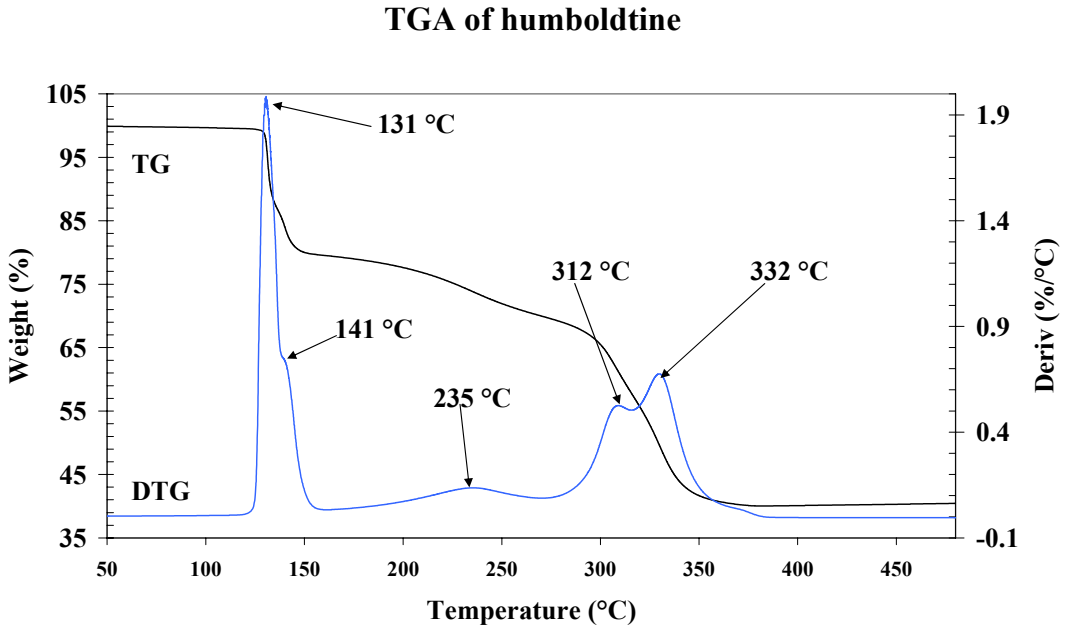


**Figure 1**

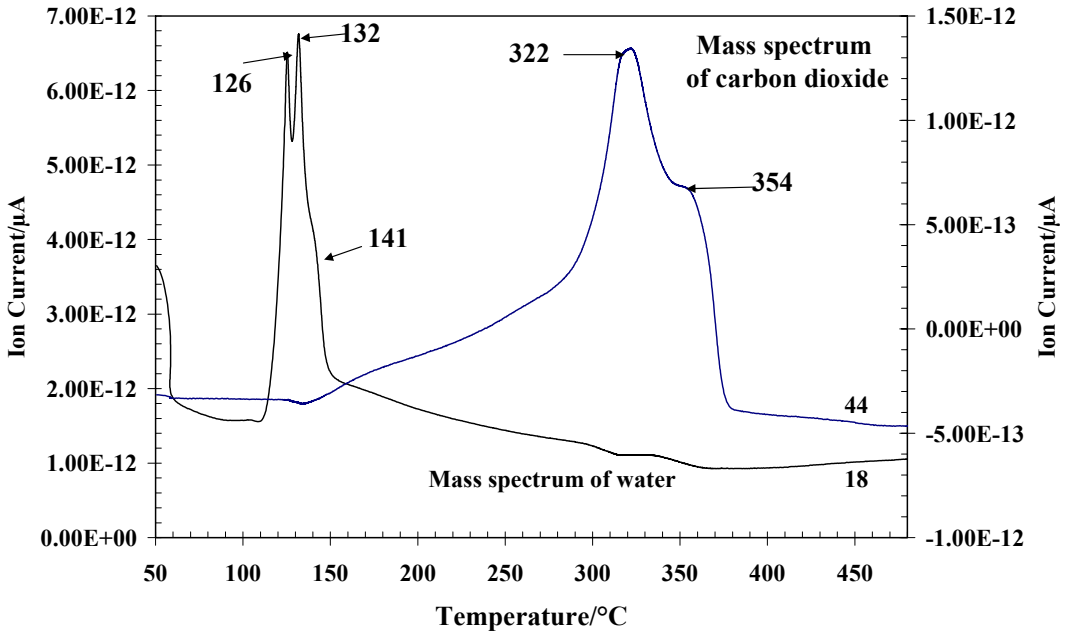


**Figure 2**

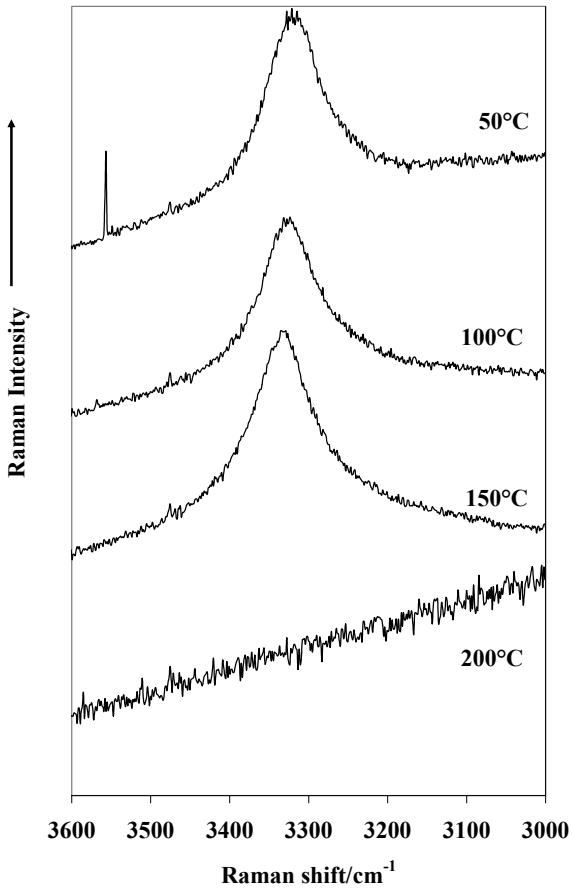


**Figure 3 Raman spectra of the hydroxyl stretching region of thermally treated humboldtine**

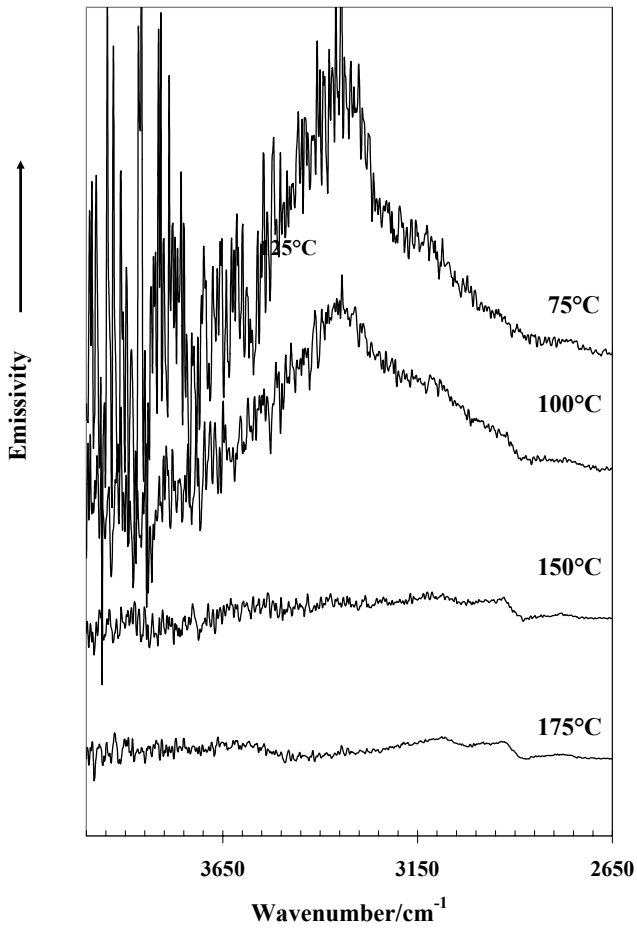


**Figure 4 Infrared emission spectra of the hydroxyl stretching region of thermally treated humboldtine**

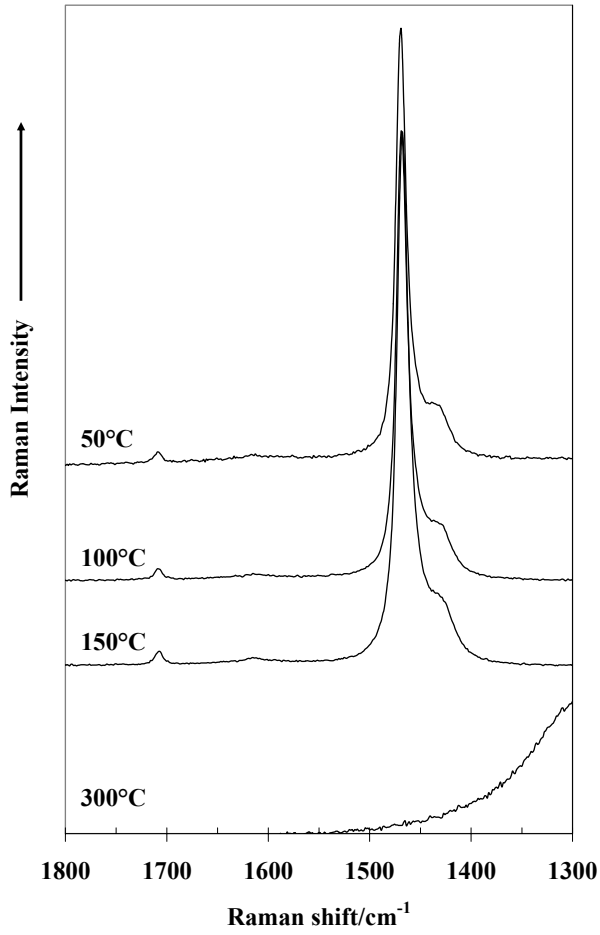


**Figure 5 Raman spectra of the 1300 to 1800 $cm^{-1}$ region of thermally treated humboldtine**

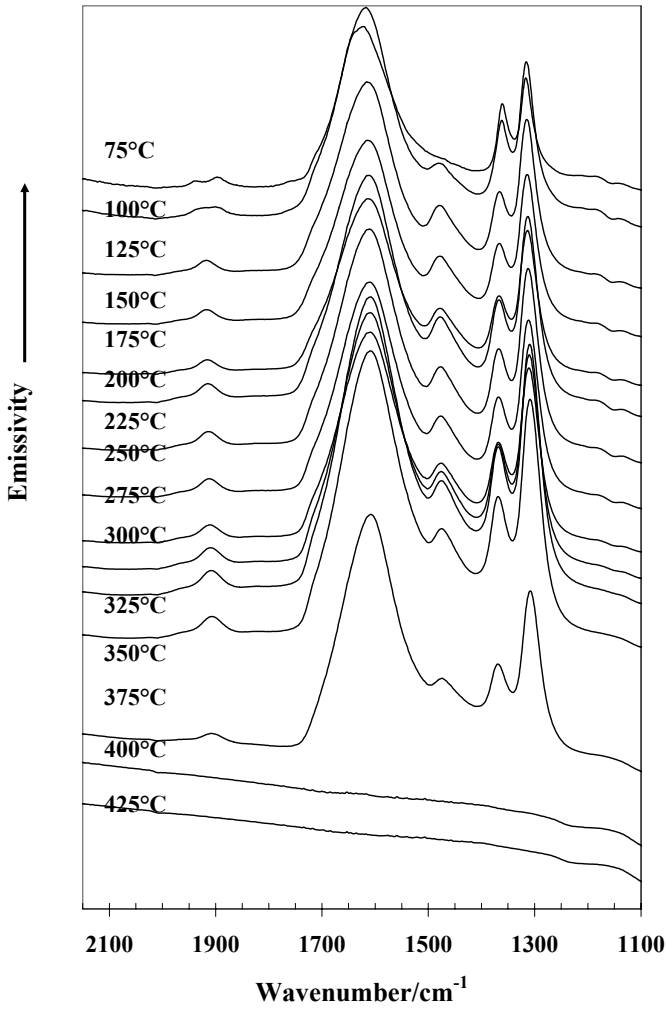


**Figure 6 Infrared emission spectra of the 1300 to 1800 $cm^{-1}$ region of thermally treated humboldtine.**

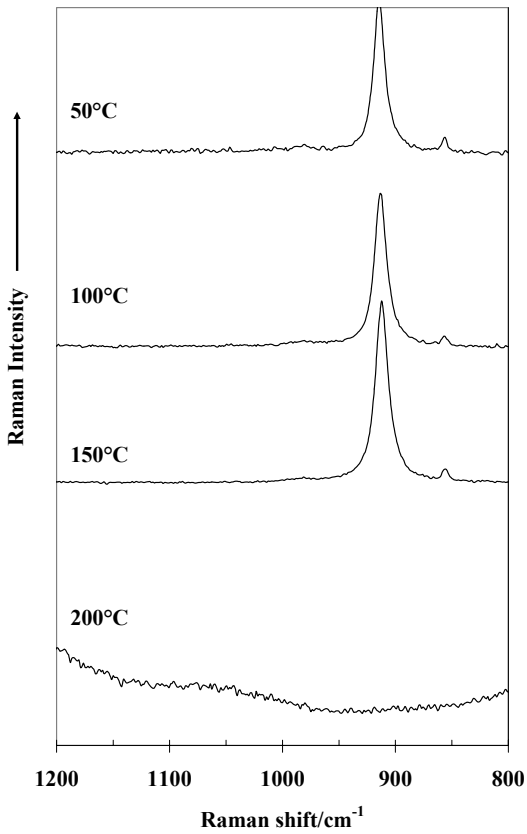


**Figure 7 Raman spectra of the 800 to 1200 $cm^{-1}$ region of thermally treated humboldtine**

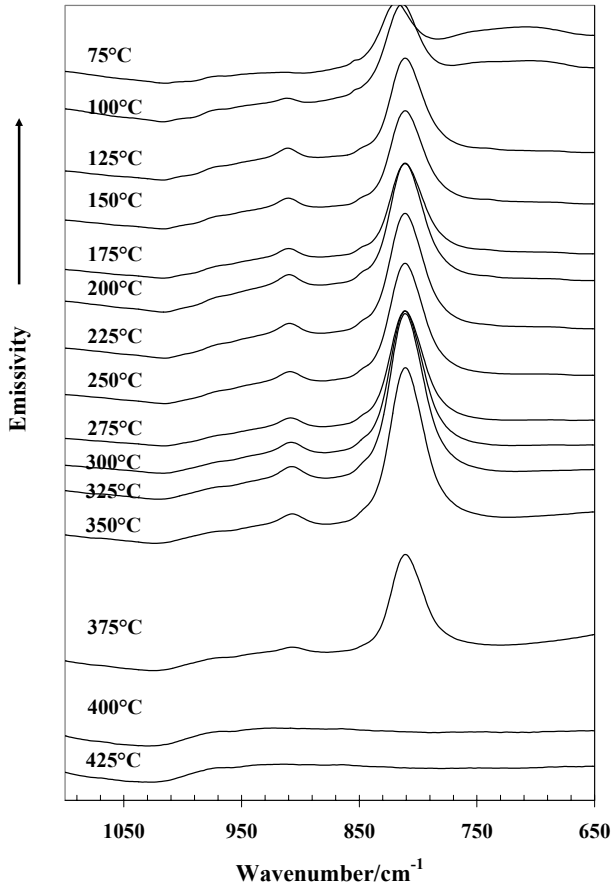


**Figure 8 Infrared emission spectra of the 650 to 1100 cm-1 region of thermally treated humboldtine.**

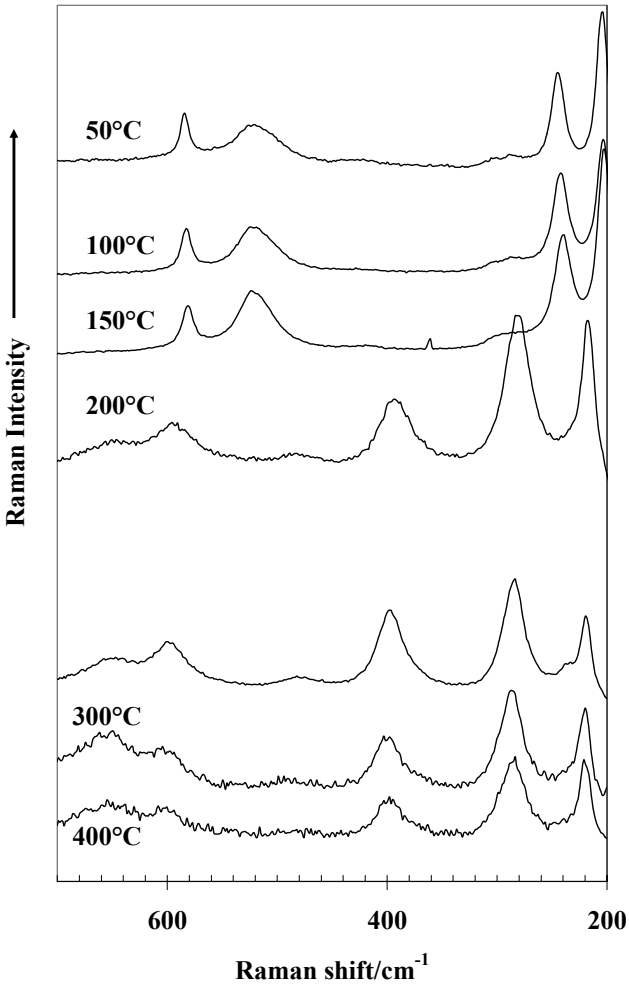


**Figure 9 Raman spectra of the 200 to 700 $cm^{-1}$ region of thermally treated humboldtine**